Discrete Maximum Principle Based on Repair Technique for Finite Element Scheme of Anisotropic Diffusion Problems

Xingding Chen[1,∗], Guangwei Yuan[2] and Yunlong Yu[3]

[1] *Department of Mathematics, School of Science, Beijing Technology and Business University, Beijing 100048, China*
[2] *LCP, Institute of Applied Physics and Computational Mathematics, P.O. Box 8009, Beijing 100088, China*
[3] *Institute of Applied Physics and Computational Mathematics, P.O. Box 8009, Beijing 100088, China*

Abstract. In this paper, we construct a global repair technique for the finite element scheme of anisotropic diffusion equations to enforce the repaired solutions satisfying the discrete maximum principle. It is an extension of the existing local repair technique. Both of the repair techniques preserve the total energy and are easy to be implemented. The numerical experiments show that these repair techniques do not destroy the accuracy of the finite element scheme, and the computational cost of the global repair technique is cheaper than the local repair technique when the diffusion tensors are highly anisotropic.

1 Introduction

Anisotropic diffusion equations appear in many physical models describing subsurface flows, heat conduction in structured materials, biological systems and plasma physics. A good diffusion scheme should be not only stable and convergent, but also possesses the mathmatical property of the physical system, such as the discrete maximum principle (DMP). The discrete maximum principle means, if the source term is non-positive, then

---

∗Corresponding author.
Email: chenxd@lsec.cc.ac.cn (X. Chen), ygw8009@sina.com (G. Yuan), yyliapcm@hotmail.com (Y. Yu)

the solution attains its maximum on the boundary. In the context of the anisotropic thermal conduction, a discrete scheme without satisfying the discrete maximum principle can lead to the violation of the entropy constraints of the second law of thermodynamics, causing heat to flow from regions of lower temperature to higher temperature. In the region of high temperature variations, this can cause the temperature to become negative. Therefore, the discrete maximum principle is an essential requirement in such diffusion processes to avoid the occurrence of unphysical phenomena.

As we know, it is very difficult to make the solution satisfy the discrete maximum principle. The classical finite volume and finite element schemes fail to satisfy the discrete maximum principle for strong anisotropic diffusion tensors or on highly distorted meshes [16–18]. The multi-point flux approximation (MPFA) method [10–12] and the mimetic finite difference (MFD) method [13,14] are second-order accurate on shape-regular meshes, but when the diffusion tensors are anisotropic or the meshes are highly distorted, these methods do not satisfy the discrete maximum principle. The diamond scheme [15], which is the so-called nine-point scheme on arbitrary quadrilateral meshes, is popular in solving diffusion equations. This method is a linear scheme and can be used on various distorted meshes for both smooth and non-smooth highly anisotropic solutions. However, this scheme is only positive-preserving and does not satisfy the discrete maximum principle. In the finite element schemes, the discrete maximum principle is satisfied by imposing severe restrictions on the choice of basis functions and on the geometric properties of the mesh. For a triangulation of acute or non-obtuse type (all angles smaller than or equal to $\pi/2$) the piecewise-linear finite element approximation of the Poisson equation satisfies DMP [4]. In the case of bilinear finite elements, it is sufficient to require that all quadrilaterals be of non-narrow type (aspect ratios smaller than or equal to $\sqrt{2}$). Recently, a nonlinear Galerkin finite element method [5] is proposed for isotropic Laplace equation on distorted meshes. Based on the repair technique and constrained optimization, the methods addressed in [2,3,7] enforce the linear finite element solution and the mixed element solution satisfying the DMP. Since the quadratic optimization is used, it is very expensive to solve the problem as the number of unknowns is increased. A constrained finite element method is described in [1], which can solve the problems with smooth coefficients very well, but is not satisfactory for the discontinuous anisotropic diffusion problems.

Compared with the existing methods, the repair technique is cheap and effective. In addition, it preserves the same total energy and accuracy as the original discrete scheme. The authors in [7, 19–21] have proposed a local repair technique to enforce the linear finite element solutions satisfying DMP. This technique repairs the out-of-bounds values one by one. Suppose a value below its minimum, we fix the value to the minimum, and the needed energy is taken from the neighborhood proportionally. If there isn't enough energy, we extend the neighborhood until enough energy is found. Then, the next value is checked and repaired if necessary. The procedure is similar to repair over-bounds values. Recently, a new repair technique [8], which is called the global repair technique, is addressed on finite volume diamond scheme for diffusion equations. In the present

paper, we will extend this global repair technique to the finite element scheme. In our method, the node values are divided into two parts: out-of-bounds node values and within-bounds node values. Firstly, all the out-of-bounds node values are repaired to the minimum (or maximum) at the same time. Then, the total needed (or excess) energy is taken from (or to) all the within-bounds node values proportionally. Comparing to the local repair technique, our method is to spread the total needed (or excess) energy through the whole domain instead of the neighborhood to preserve the same total energy. The underlying idea of our method is similar to the repair technique proposed in [20,21], which is addressed in a different form.

The outline of this paper is as follows. In Section 2, we give the model problem and briefly review the maximum principle and the discrete maximum principle. In Section 3, we describe the local repair technique, and extend the global repair technique to the finite element scheme. Numerical experiments will be presented in Section 4 which is followed by a summary and conclusions in Section 5.

2 The model problem and the maximum principle

In this section, we consider the stationary diffusion problem with the Dirichlet boundary condition:

$$-div\cdot(\kappa\nabla u)=f \qquad \text{in } \Omega, \tag{2.1a}$$
$$u(x)=\psi(x) \qquad \text{on } \partial\Omega, \tag{2.1b}$$

where κ is a 2×2 symmetric positive defined diffusion tensor, f is a source term, and Ω is an open bounded polygonal set of $\mathbb{R}^2$ with boundary $\partial\Omega$.

The maximum principle is a basic and important feature of second-order elliptic equations. It can be described as follows. If $f(x)\leq0$ for all $x\in\Omega$, then $u(x)$ has the maximum on the boundary, that is

$$u(x)\leq\max_{x\in\partial\Omega}\psi(x), \quad \forall x\in\Omega. \tag{2.2}$$

If $f(x)\geq0$ for all $x\in\Omega$, then $u(x)$ has the minimum on the boundary, so that

$$u(x)\geq\min_{x\in\partial\Omega}\psi(x), \quad \forall x\in\Omega. \tag{2.3}$$

We use the finite element method to discretize (2.1a)-(2.1b) on triangular meshes, the discrete values of $u(x)$, $f(x)$ at the mesh node K are denoted by U_K and f_K. It is well known that under some assumptions about the mesh regularity, the solution of the standard finite element method converges to the solution of the Dirichlet problem with mesh refinements [6]. The discrete version of the maximum principle (2.2) for non-positive sources ($\forall K, f_K\leq0$) states that,

$$U_K\leq\max_{J\in\partial\Omega}\psi_J, \quad \forall K, \tag{2.4}$$

where $J \in \partial\Omega$ is the boundary node, and the discrete Dirichlet boundary condition is given by $\psi_J = \psi(J)$.

The discrete version of the minimum principle (2.3) for the non-negative sources ($\forall K$, $f_K \geq 0$) states that,

$$U_K \geq \min_{J \in \partial\Omega} \psi_J, \quad \forall K. \tag{2.5}$$

3   Enforcing the discrete maximum principle

The repair technique is a kind of posteriori corrections of the discrete solution, and it allows to correct the discrete solution in such a way that the total discrete energy is preserved. In this section, two repair techniques will be considered for the finite element scheme. One is the local repair technique [7], and the other is the global repair technique, which was firstly proposed in [8] for the finite volume diamond scheme. In this section, we will extend the global repair technique to the finite element scheme, and describe both of the repair techniques in details.

3.1   Notions of the energy

In the case of heat diffusion equations, u is the temperature and the discretization of the total energy $\int_\Omega u dx$ is defined as

$$E(U) = \sum_{K \in \mathcal{J}} U_K V_K, \tag{3.1}$$

where $\mathcal{J}$ is the set of mesh nodes, and V_K is the volume associated with the node K defined as one third of the sum of areas of all triangles which have the node K as one of their vertices. In many applications, it is important to preserve the conservation of total energy when modifying the discrete solution to satisfy the discrete maximum principle. Define $U_{\min} = \min_{J \in \partial\Omega} \psi_J$ as the minimum on the boundary. Define U^u as the unrepaired solution and U^r as the repaired solution. The total energy of the unrepaired solution is $E(U^u)$, and we require that the repaired solution preserves the same total energy, that is,

$$E(U^r) = E(U^u) = \sum_K U_K^u V_K. \tag{3.2}$$

3.2   Local repair technique

Following [7], we repair the node values which violate the discrete maximum principle by redistributing the heat energy to and from their neighbors so that (3.2) remains valid. For simplicity, we drop the superscript u denoting the unrepaired solution. We denote by $\mathcal{N}(K)$ the set of nodes neighboring the node K (each neighboring node defines one edge connecting this node with the node K). Assume that $U_K < U_{\min}$, to correct the violation of the lower bound on the node K, we have to add the needed energy $E_K = -(U_K - U_{\min}) V_K$

to the node K. For all neighboring nodes L of $\mathcal{N}(K)$, the available energy at node L is $E_L^a = \max(0, (U_L - U_{\min})V_L)$, which can be taken out and given to the node K. So, the total available energy in $\mathcal{N}(K)$ is

$$E^a = \sum_{L \in \mathcal{N}(K)} E_L^a. \tag{3.3}$$

Now, if $E^a \geq E_K$, we have enough available energy to correct the temperature on the node K to the minimal value $U_{\min}$. Set $U_K^r = U_{\min}$ and take out the needed energy E_K from $\mathcal{N}(K)$ in proportion to what they can give, which leads to the following formula

$$U_L^r = U_L - \frac{E_L^a \frac{E_K}{E^a}}{V_L}. \tag{3.4}$$

On the other hand, if the availbale energy E^a is less than the needed energy E_K, we extend the neighborhood $\mathcal{N}(K)$ by the neighbors of all nodes from $\mathcal{N}(K)$ and repeat the outline procedure.

When the upper bound on the solution is not valid, the repair of the temperature violating the upper bound proceeds in a similar way as that described above.

3.3 Global repair technique

In this subsection, we extend the global repair technique [8], which was firstly proposed for the finite volume diamond scheme, to the finite element scheme. We divide the mesh nodes set $\mathcal{J}$ into two parts: $\mathcal{J}_p = \{K : U_K \geq U_{\min}\}$ and $\mathcal{J}_n = \{K : U_K < U_{\min}\}$. Define $E_p = \sum_{K \in \mathcal{J}_p}(U_K - U_{\min})V_K$ as the total available energy, and $E_n = -\sum_{K \in \mathcal{J}_n}(U_K - U_{\min})V_K$ as the total needed energy. For each $K \in \mathcal{J}$, let

$$E_K = \begin{cases} (U_k - U_{\min})V_K, & K \in \mathcal{J}_p, \\ -(U_K - U_{\min})V_K, & K \in \mathcal{J}_n, \end{cases} \tag{3.5}$$

then

$$E_p = \sum_{K \in \mathcal{J}_p} E_K = \sum_{K \in \mathcal{J}_p}(U_K - U_{\min})V_K, \quad E_n = \sum_{K \in \mathcal{J}_n} E_K = -\sum_{K \in \mathcal{J}_n}(U_K - U_{\min})V_K. \tag{3.6}$$

If $E_p < E_n$, then the total energy in the whole domain becomes negative and the numerical solution is non-physical. In such case, any repair technique will keep the total energy being negative, so it is unnecessary to proceed the repair process, and we have to take other suitable methods to solve the diffusion problems.

If $E_p \geq E_n$, then the total available energy in the whole domain is greater than the total needed energy. We can take the energy from $\mathcal{J}_p$ to compensate the deficiency of the energy in the set $\mathcal{J}_n$.

For the repaired solution, it is required that $U_K^r \geq U_{\min}$, so we set

$$U_K^r = U_{\min}, \quad \forall K \in \mathcal{J}_n, \tag{3.7}$$

and

$$U_K^r = U_K - \frac{E_K \frac{E_n}{E_p}}{V_K}, \quad \forall K \in \mathcal{J}_p. \tag{3.8}$$

Because $E_p \geq E_n$, there holds

$$U_K^r \geq U_K - \frac{E_K}{V_K} = U_{\min}, \quad \forall K \in \mathcal{J}_p. \tag{3.9}$$

Following the proof of Theorem 4.1 in [8], we can deduce that this global repair technique also preserves the same total energy as the unrepaired solution, that is $E(U) = E(U^r)$.

When the upper bound on the solution (2.4) is not valid, the repair of the temperature violating the upper bound proceeds in a similiar way as that described above.

As we mentioned above that when the total available energy is greater than the total needed one, the repair technique can proceed with no problem. However, when the total available energy is less than the total needed one, the local repair technique will result in a dead circle and has to terminate, see details in [7]. But, in the context of the global repair technique, a necessary condition to enable the repair procedure can be derived, that is $E_p \geq E_n$.

4   Numerical experiments

In this section, we apply both of the repair techniques to the diffusion problems. In the Subsection 4.1-4.3, we consider the linear steady diffusion model (2.1a), (2.1b). In the Subsection 4.4, we consider the nonlinear steady diffusion model, while the time-dependent nonlinear diffusion problem is addressed in the Subsection 4.5.

The computational domain is the unit square $[0,1] \times [0,1]$. The standard linear triangular finite elements are used, we adopt two different meshes: uniform meshes and distorted meshes. The distorted mesh is constructed from the uniform mesh with mesh size h by random perturbations of the internal nodes (x,y)

$$x := x + \alpha \eta_x h, \quad y := y + \alpha \eta_y h,$$

where η_x and η_y are random numbers with values in the range from -0.5 to 0.5. The parameter $\alpha \in [0,1]$ quantifies the degree of distortion. The default value $\alpha = 0.4$ is adopted to introduce sufficiently strong grid deformations without tangling. When the mesh is refined, we proceed the above disturbance on the relatted uniform mesh.

We use the discrete L^2-norm and L^∞-norm to evaluate the approximation errors. For the exact solution u, define the following L^2-norm error

$$\varepsilon_2 = \left[\sum_{K \in \mathcal{J}} (U_K - u(K))^2 V_K \right]^{\frac{1}{2}},$$

and the L^∞-norm error

$$\varepsilon_\infty = \max_{K \in \mathcal{J}} |U_K - u(K)|.$$

4.1 Anisotropic medium (Test Problem 1)

Consider the homogeneous Dirichlet boundary condition, i.e., $\psi(x)=0$. The source function is taken as follows:

$$f = \begin{cases} 1, & \text{if } (x,y) \in [3/8, 5/8]^2, \\ 0, & \text{otherwise.} \end{cases}$$

The diffusion tensor is given by

$$\kappa = \begin{pmatrix} y^2 + \epsilon x^2 & -(1-\epsilon)xy \\ -(1-\epsilon)xy & \epsilon y^2 + x^2 \end{pmatrix}.$$

In this test, three values of the parameter $\epsilon = 0.05$, $\epsilon = 0.01$ and $\epsilon = 0.001$ are specified, and we use the uniform triangular meshes.

The unrepaired solutions of this problem for all three parameters have some negative values, the minimal values of the unrepaired solutions on refined meshes are presented in Table 1. To quantify how badly the solutions are, we give the ratio of the areas where the solutions are negative and the area of the whole domain.

The exact solution of this problem is not known, so for convergence study we use the reference unrepaired solution computed on the finest mesh with mesh scale $N = 128 \times 128$.

Table 1: Test Problem 1. Minimal of unrepaired solutions and the percentage of nodes that have negative temperature under different parameters (denoted as % of negative nodes).

cells	$\epsilon = 0.05$		$\epsilon = 0.01$		$\epsilon = 0.001$	
	Minimal	negative (%)	Minimal	negative (%)	Minimal	negative (%)
8×8	-6.6681e-007	1.23	-1.1771e-003	6.17	-1.7516e-003	14.81
16×16	-1.6138e-007	0.69	-5.6343e-004	15.22	-1.8964e-003	25.25
32×32	-3.8309e-008	0.36	-6.4127e-005	7.80	-1.2213e-003	30.39
64×64	-9.1877e-009	0.44	-3.9338e-005	4.99	-7.3838e-004	33.15

Table 2: Test Problem 1. The L^2-norm error when $\epsilon = 0.01$, and the convergence order.

cells	Unrepair		Local repair		Global repair	
	ε_2	Order	ε_2	Order	ε_2	Order
8×8	4.8248e-003	-	4.7850e-003	-	4.8593e-003	-
16×16	1.6730e-003	1.5280	1.6689e-003	1.5196	1.6839e-003	1.5289
32×32	4.9900e-004	1.7453	4.9892e-004	1.7593	4.9988e-004	1.7522
64×64	1.1486e-004	2.1192	1.1486e-004	2.1189	1.1486e-004	2.1217

Table 3: Test Problem 1. The L^∞-norm error when $\epsilon = 0.01$, and the convergence order.

cells	Unrepair		Local repair		Global repair	
	ε_∞	Order	ε_∞	Order	ε_∞	Order
8×8	1.5094e-002	-	1.5094e-002	-	1.5334e-002	-
16×16	6.5022e-003	1.2150	6.5022e-003	1.2150	6.5894e-003	1.2185
32×32	2.3650e-003	1.4591	2.3650e-003	1.4591	2.3732e-003	1.4733
64×64	6.4490e-004	1.8747	6.4450e-004	1.8756	6.4449e-004	1.8806

Table 4: Test Problem 1. Numbers of repair for the global and local repair techniques, mesh scale is $N=64\times64$.

negative (%)	$\epsilon=0.05$	$\epsilon=0.01$	$\epsilon=0.001$
	0.44	4.99	33.15
Number of local repair	114	1266	8406
Number of global repair	4206	4014	2824

Table 5: Test Problem 1. Numbers of repair for the global and local repair techniques, the parameter $\epsilon=0.001$.

negative (%)	$N=16$	$N=32$	$N=64$
	25.25	30.39	33.15
Number of local repair	438	1986	8406
Number of global repair	216	758	2824

The convergence results are presented in Table 2 and Table 3. We can see that both of the repair techniques do converge, and the L^2-norm and L^∞-norm errors after repairing are about the same as the original finite element method. Hence, the repair techniques do not destroy the convergence.

We compare the global repair technique with the local repair technique. When the formula (3.4) or (3.8) is computed once, the number of repairs add one. The compared results are shown in Table 4 and Table 5. From the tables, we can see, when the percentage of nodes that give negative temperature becomes large, the number of global repair become smaller than the local repair remarkably.

4.2 Heterogenous diffusion tensor (Test Problem 2)

Consider the case of strong jumps of full diffusion tensors across mesh edges. Assume $\psi(x)=0$, and the forcing term is

$$f=\begin{cases} 1, & \text{if } (x,y)\in[7/18,11/18]^2, \\ 0, & \text{otherwise}. \end{cases}$$

The domain Ω is partitioned into four square subdomains $\Omega_i, i=1,\cdots,4$. The diffusion tensor is given by

$$\kappa=\begin{pmatrix} \cos\theta & \sin\theta \\ -\sin\theta & \cos\theta \end{pmatrix}\begin{pmatrix} k_1 & 0 \\ 0 & k_2 \end{pmatrix}\begin{pmatrix} \cos\theta & -\sin\theta \\ \sin\theta & \cos\theta \end{pmatrix}.$$

Case 1: we fix the anisotropic ratio by setting $k_1=1000$, $k_2=1$ and vary only the parameter θ, see Fig. 1(a). Case 2: we use different parameters k_1, k_2 and θ on different subdomains, see Fig. 1(b). The computational mesh is the uniform triangular mesh.

The minimal values of the unrepaired solutions and the ratio of negative values are presented on Table 6. The solution colormaps of Case 1 and Case 2 are given in Fig. 2. From this figure, we can see that both of the repair techniques enforce the finite element solutions satisfying the discrete maximum principle.

Table 6: Test Problem 2. Minimal of unrepaired solutions and the percentage of nodes that have negative temperature under different parameters (denoted as % of negative nodes).

cells	Case 1		Case 2	
	Minimal	negative (%)	Minimal	negative (%)
8×8	-2.8007e-006	7.41	-5.1343e-005	27.16
16×16	-7.6743e-006	33.22	-5.1717e-004	31.83
32×32	-1.9284e-005	39.67	-4.1800e-005	20.75
64×64	-2.8121e-005	42.27	-1.9009e-005	16.52

Table 7: Test Problem 2. Case 1, numbers of repair for the global and local repair techniques.

negative (%)	$N=16$ 33.22	$N=32$ 39.67	$N=64$ 42.27
Number of local repair	576	2592	10916
Number of global repair	193	657	2439

Table 8: Test Problem 2. Case 2, numbers of repair for the global and local repair techniques.

negative (%)	$N=16$ 31.83	$N=32$ 20.75	$N=64$ 16.52
Number of local repair	552	1356	4188
Number of global repair	197	863	3527

The number of repairs for the two repair techniques are presented in Table 7 and Table 8. We can see, when the percentage of nodes that give negative temperature becomes large, the number of global repair is smaller than the local repair.

Figure 1: Parameters in Test Problem 2.

4.3   Non-smooth anisotropic solution (Test Problem 3)

Consider the Dirichlet boundary conditions: when $x=0$ or $x=1$, $\psi(x)=2.0$; when $y=0$ or $y=1$, $\psi(x)=0.0$. The four corners of the domain satisfy $\psi(x)=0$. The forcing function
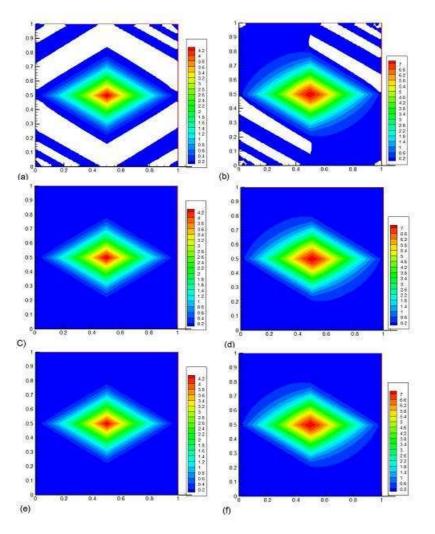
Figure 2: Test Problem 2. Solution colormaps of Case 1 (left) and Case 2 (right) of (a), (b) unrepaired; (c), (d) local repaired; (e), (f) global repaired. Mesh scale is 64×64. The regions that have negative temperature are indicated in white.

is taken as $f = 0$. The diffusion tensor is given by

$$\kappa = \begin{pmatrix} \cos\theta & \sin\theta \\ -\sin\theta & \cos\theta \end{pmatrix} \begin{pmatrix} k_1 & 0 \\ 0 & k_2 \end{pmatrix} \begin{pmatrix} \cos\theta & -\sin\theta \\ \sin\theta & \cos\theta \end{pmatrix}.$$

We take $k_1 = 1$, $k_2 = 10^3$, 10^4, 10^5, and $\theta = \pi/6$, and the problem is solved on the distorted triangular meshes.

The convergence results are shown in Table 10 and Table 11. We can see that both of the repair techniques do not destroy the L^2-norm and L^∞-norm convergences. In Table 9, we compare the repair numbers between the local and the global repaire techniques. The numerical solution profiles and the colormaps are shown in Fig. 3.

Table 9: Test Problem 3. Numbers of repair for the global and local repair techniques, mesh scale is $N=64\times64$.

violate DMP(%)	$k_2=10^3$	$k_2=10^4$	$k_2=10^5$
	16.68	17.58	17.63
Number of local repair	4230	4458	4470
Number of global repair	3520	3482	3480

Table 10: Test Problem 3. The L^2-norm error when $k_1=1$, $k_2=10^3$ and the convergence order.

cells	Unrepair		Local repair		Global repair	
	ε_2	Order	ε_2	Order	ε_2	Order
8×8	2.1277e-001	-	2.1277e-001	-	2.1277e-001	-
16×16	1.4563e-001	0.5470	1.4563e-001	0.5470	1.4563e-001	0.5470
32×32	8.8668e-002	0.7158	8.8389e-002	0.7207	8.8917e-002	0.7112
64×64	4.2959e-002	1.0455	4.2588e-002	1.0534	4.3838e-002	1.0203

Table 11: Test Problem 3. The L^∞-norm error when $k_1=1, k_2=10^3$ and the convergence order.

cells	Unrepair		Local repair		Global repair	
	ε_∞	Order	ε_∞	Order	ε_∞	Order
8×8	5.6869e-001	-	5.6867e-001	-	5.6867e-001	-
16×16	4.4338e-001	0.3591	4.4338e-001	0.3590	4.4338e-001	0.3590
32×32	3.1625e-001	0.4875	3.1625e-001	0.4875	3.1525e-001	0.4920
64×64	2.0849e-001	0.6011	2.0849e-001	0.6011	2.0187e-001	0.6431

4.4   The nonlinear diffusion problem (Test Problem 4)

Consider the following nonlinear diffusion problem with Dirichlet boundary condition on the domain $\Omega=[0,1]\times[0,1]$:

$$\begin{cases} -div(\kappa(u)\nabla u)=f & \text{in } \Omega, \\ u=0, & \text{on } \partial\Omega, \end{cases} \tag{4.1}$$

where $\kappa(u)$ is the diffusion tensor associated with u, f is the source term.

As usual, we use the Picard method to solve the discrete nonlinear system of problem (4.1). After the finite element solution is gotten, we apply the local and global repair techniques to enforce the solution satisfying the discrete maximum principle.

Set

$$f=\begin{cases} 1000, & (x,y)\in[7/18,11/18]^2, \\ 0, & \text{otherwise.} \end{cases}$$

The diffusion tensor is

$$\kappa(u)=\begin{pmatrix} \cos\theta & \sin\theta \\ -\sin\theta & \cos\theta \end{pmatrix}\begin{pmatrix} 1+u & 0 \\ 0 & \epsilon(1+u) \end{pmatrix}\begin{pmatrix} \cos\theta & -\sin\theta \\ \sin\theta & \cos\theta \end{pmatrix}.$$
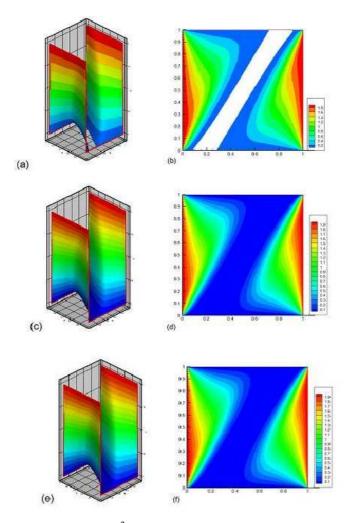
Figure 3: Test Problem 3. $k_1 = 1$, $k_2 = 10^3$, distorted triangular mesh. Solution profiles (left) and solution colormaps (right) of (a), (b) unrepaired; (c), (d) local repaired; (e), (f) global repaired. Mesh scale is 64×64. The regions that violate the DMP are indicated in white.

Choose $\epsilon = 10^2, 10^3, 10^4$ and $\theta = \pi/6$, we solve the nonlinear problem on the uniform triangular mesh. The exact solution of this problem is not known, so for convergence study we use the reference unrepaired solution computed on the finest mesh with mesh scale $N = 128 \times 128$.

The unrepaired solutions of this problem for all three parameters have some negative values, the minimal values and the ratio of negative values of the unrepaired solution on refined meshes are presented in Table 12.

The convergence results are presented in Table 13 and Table 14. From the L^2-norm and L^∞-norm errors of the repaired solutions, we can see that both of the repair techniques do not destroy the convergence. We compare the global repair technique with the local

Table 12: Test Problem 4. Minimal of unrepaired solutions and the percentage of nodes that have negative temperature under different parameters (denoted as % of negative nodes).

cells	$\epsilon=10^2$		$\epsilon=10^3$		$\epsilon=10^4$	
	Minimal	negative (%)	Minimal	negative (%)	Minimal	negative (%)
8×8	-3.6743e-003	4.93	-4.5521e-004	4.93	-4.6521e-005	7.40
16×16	-5.0403e-003	17.99	-7.4394e-004	20.76	-7.7103e-005	20.76
32×32	-4.8529e-003	24.97	-1.1036e-003	27.91	-1.1946e-004	28.28
64×64	-1.9240e-003	26.93	-1.1001e-003	32.61	-1.2767e-004	32.94

Table 13: Test Problem 4. The L^2-norm error when $\epsilon=10^3$, and the convergence order.

cells	Unrepair		Local repair		Global repair	
	ε_2	Order	ε_2	Order	ε_2	Order
8×8	8.2783e-003	-	8.2682e-003	-	8.2821e-003	-
16×16	6.7787e-003	0.2883	6.7680e-003	0.2888	6.8667e-003	0.2703
32×32	3.5394e-003	0.9375	3.5212e-003	0.9426	3.6689e-003	0.9042
64×64	1.4476e-003	1.2898	1.4434e-003	1.2865	1.6269e-003	1.1732

Table 14: Test Problem 4. The L^∞-norm error when $\epsilon=10^3$, and the convergence order.

cells	Unrepair		Local repair		Global repair	
	ε_∞	Order	ε_∞	Order	ε_∞	Order
8×8	2.3467e-002	-	2.3467e-002	-	2.3572e-002	-
16×16	2.3913e-002	-0.0271	2.3913e-002	-0.0271	2.4397e-002	-0.0496
32×32	1.1538e-002	1.0514	1.1538e-002	1.0514	1.2390e-002	0.9775
64×64	4.8933e-003	1.2375	4.8933e-003	1.2375	5.6403e-003	1.1353

Table 15: Test Problem 4. Numbers of repair for the global and local repair techniques, mesh scale is $N=64\times64$.

negative (%)	$\epsilon=10^2$	$\epsilon=10^3$	$\epsilon=10^4$
	26.93	32.61	32.94
Number of local repair	6828	8268	8352
Number of global repair	3087	2847	2833

repair technique, the results are shown in Table 15. The numerical solution profiles and the colormaps are shown in Fig. 4.

4.5 The time-dependent diffusion problem (Test Problem 5)

Consider the following time-dependent nonlinear diffusion problem on the domain $\Omega=[0,1]\times[0,1]$:

$$
\begin{cases}
\dfrac{\partial u}{\partial t}-div(\kappa(u)\nabla u)=f & \text{in } \Omega, \\[2mm]
u(x,y,t)=10\exp\left(\dfrac{a^2(x-c)^2+b^2(y-c)^2}{a^2(x-c)^2+b^2(y-c)^2-a^2b^2}\right), & a^2(x-c)^2+b^2(y-c)^2<a^2b^2, \\[2mm]
u(x,y,t)=0, & a^2(x-c)^2+b^2(y-c)^2\geq a^2b^2, \\[2mm]
K(u)\dfrac{\partial}{\partial \mathbf{n}}u(x,y,t)=0, & (x,y)\in\partial\Omega, \quad t\in(0,T],
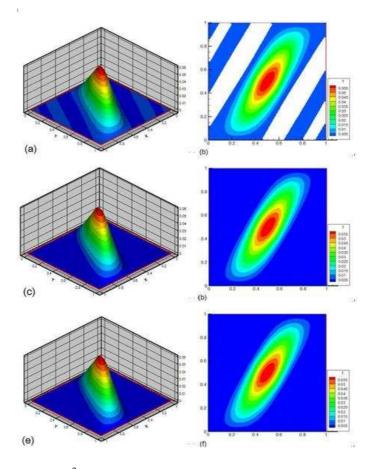\end{cases}
\tag{4.2}
$$

Figure 4: Test Problem 4. $\epsilon = 10^3$, solution profiles (left) and solution colormaps (right) of (a), (b) unrepaired; (c), (d) local repaired; (e), (f) global repaired. Mesh scale is 64×64. The regions that have negative temperature are indicated in white.

where **n** is the unit outward normal vector on $\partial\Omega$, the parameters $a = b = 0.1$, $c = 0.5$.

We use the unconditionally stable connotative scheme to discrete the time. In each time step, the Picard method is adopted to solve the relatted nonlinear system. After the finite element solution of (4.2) is gotten, we apply both of the local and global repair techniques to enforce the solution satisfying the discrete maximum principle.

Set the time $T = 0.001$, and choose the time interval $\Delta t = 10^{-6}$. The force term is

$$f = \begin{cases} 1000, & (x,y) \in [7/18, 11/18]^2, \\ 0, & \text{otherwise}. \end{cases}$$

The diffusion tensor is

$$\kappa(u) = \begin{pmatrix} \cos\theta & \sin\theta \\ -\sin\theta & \cos\theta \end{pmatrix} \begin{pmatrix} 1+u & 0 \\ 0 & \epsilon(1+u) \end{pmatrix} \begin{pmatrix} \cos\theta & -\sin\theta \\ \sin\theta & \cos\theta \end{pmatrix},$$

Table 16: Test Problem 5. The L^2-norm error and the convergence order.

cells	Unrepair		Local repair		Global repair	
	ε_2	Order	ε_2	Order	ε_2	Order
8×8	0.2207	-	0.2191	-	0.2201	-
16×16	0.2024	0.1248	0.1996	0.1344	0.2025	0.1202
32×32	0.1568	0.3682	0.1552	0.3629	0.1591	0.3479
64×64	0.1034	0.6006	0.1015	0.6126	0.1069	0.5736
128×128	4.5552e-2	1.1826	4.4556e-2	1.1556	4.9229e-2	1.1186

Table 17: Test Problem 5. The L^∞-norm error and the convergence order.

cells	Unrepair		Local repair		Global repair	
	ε_∞	Order	ε_∞	Order	ε_∞	Order
8×8	0.4607	-	0.4607	-	0.4676	-
16×16	0.4440	0.0532	0.4440	0.0532	0.4620	0.0173
32×32	0.3404	0.3833	0.3404	0.3833	0.3636	0.3455
64×64	0.2236	0.6063	0.2236	0.6063	0.2517	0.5306
128×128	9.5903e-2	1.2213	9.5903e-2	1.2213	0.1199	1.0698

Table 18: Test Problem 5. Numbers of repair for the global and local repair techniques under different mesh scales.

	$N=32$	$N=64$	$N=128$
negative (%)	27.18	31.85	34.57
Number of local repair	1664	7890	34072
Number of global repair	793	2879	10887

where $\epsilon = 1000$, $\theta = \pi/6$. The problem is solved on the distorted triangular mesh. For the exact solution is unknown, the numerical solution on the mesh scale $N = 256 \times 256$ is taken as the reference solution.

The convergence results are presented in Table 16 and Table 17. From the L^2-norm and L^∞-norm errors of the repaired solutions, we can see both of the repair techniques do not destroy the convergence.
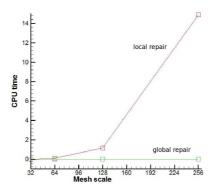

Figure 5: Test Problem 5. The CPU time of the local and global repair techniques under different mesh scale.
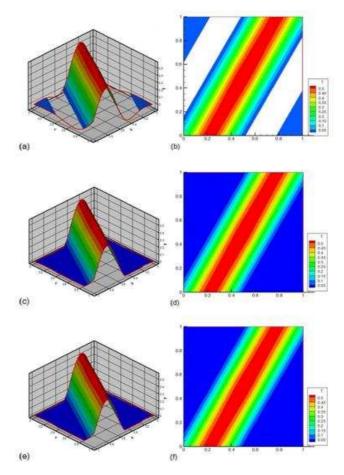
Figure 6: Test Problem 5. Solution profiles (left) and solution colormaps (right) of (a), (b) unrepaired; (c), (d) local repaired; (e), (f) global repaired. Mesh scale is 64×64. The regions that have negative temperature are indicated in white.

We compare the global repair technique with the local repair technique, the results are shown in Table 18. The CPU time of the two repair techniques is presented in Fig. 5. We can see, it costs very little CPU time to implement the repair procedures in this numerical experiment. But, when the mesh scale is increased, the CPU time of the local repair technique increases remarkably, while the CPU time of the global repair technique increases very slowly. The numerical solution profiles and the colormaps are shown in Fig. 6.

5　Conclusions

In this paper, we extend the global repair technique [8] to the finite element scheme and make the repaired solutions satisfy the discrete maximum principle. It is showed that both of the repair techniques do not destroy the convergence of the original finite element

method. When the diffusion tensors are highly anisotropic, the computational cost of the global repair technique is cheaper than the local repair technique.

Acknowledgments

References

[1] D. KUZMIN, M. SHASHKOV AND D. SVYATSKIY, *A constrained finite element method satisfying the discrete maximum priciple for anisotropic diffusion problems*, J. Comput. Phys., 228 (2009), pp. 3448–3463.

[2] H. NAGARAJAN AND K. NAKSHATRALA, *Enforcing the non-negativity constraint and maximum principles for diffusion with decay on general computational grids*, Int. J. Numer. Meth. Flu., 67 (2011), pp. 820–847.

[3] K. NAKSHATRALA AND A. VALOCCHI, *Non-negative mixed finite element formulation for a tensorial diffusion equation*, J. Comput. Phy., 228 (2009), pp. 6726–6752.

[4] P. G. CIARLET AND P. A. RAVIART, *Maximum principle and convergence for the finite element method*, Comput. Meth. Appl. Mech. Eng., 2 (1973), pp. 17–31.

[5] E. BURMAN AND A. ERN, *Discrete maximum priciple for Galerkin approximation of the Laplace operator on arbitrary meshes*, Comptes Rendus Mathematique Academie des Sciences, Paris, 338 (2004), pp. 641–646.

[6] P. G. CIARLET, *Basic error estimates for elliptic problems*, in: P. G. Ciarlet and J. L. Lions (Eds), Handbook of Numerical Analysis, Volume II: Finite Element Methods (Part 1), Elsevier, 1990.

[7] R. LISKA AND M. SHASHKOV, *Enforcing the discrete maximum principle for linear finite element solutions of second-order elliptic problems*, Commun. Comput. Phys., 3(4) (2008), pp. 852–877.

[8] S. WANG, GW. YUAN, YH. LI AND ZQ. SHENG, *Discrete maximum principle based on repair technique for diamond type scheme of diffusion problems*, Int. J. Numer. Meth. Flu., 70 (2012), pp. 1188–1205.

[9] WZ. HUANG AND A. KAPPEN, *A study of cell-center finite volume methods for diffusion equations*, Mathematics Research Report, University of Kansas, Lawrence KS66045, 98-10-01.

[10] I. AAVATSMARK, *An introduction to multipoint flux approximations for quadrilateral grids*, Comput. Geosciences, 6 (2002), pp. 405–432.

[11] H. FRIIS AND M. EWARDS, *A family of m_p finite-volume schemes with full presseure support for general tensor oressure equation on cell-centered triangular grids*, J. Comput. Phys., 230 (2011), pp. 205–231.

[12] J. NORDBOTTEN AND G. EIGESTAD, *Discritization on quadrilateral grids with improved mono-toncity properties*, J. Comput. Phys., 203 (2005), pp. 744–760.

[13] K. LIPNIKOV, M. SHASHKOV AND D. SVYATSKIY, *The mimetic finite difference discretization of diffusion problem on unstructured polyhedral meshes*, J. Comput. Phys., 211 (2006), pp. 473–491.

[14] K. LIPNIKOV, M. SHASHKOV AND I. YOTOV, *Local flux mimetic finite difference methods*, Numer. Math., 112 (2009), pp. 115–152.

[15] GW. YUAN AND ZQ. SHENG, *Monotone finite volume schemes for diffusion equations on polygonal meshes*, J. Comput. Phy., 227 (2008), pp. 6288–6312.

[16] A. DRAGANESCU, T. F. DUPONT AND L. R. SCOTT, *Failure of the discrete maximum principle for an elliptic finite element problem*, Math. Comput., 74(249) (2004), pp. 1–23.

[17] H. HOTEIT, R. MOSE, B. PHILIPPE. PH. ACKERER AND J. ERHEL, *The maximum principle violations of the mixed-hybrid finite-element method applied to diffusion equations*, Numer. Meth. Eng., 55(12) (2002), pp. 1373–1390.

[18] J. M. NORDBOTTEN, I. AAVATSMARK AND G. T. EIGESTAD, *Monotonicity of control volume methods*, Numer. Math., 106 (2007), pp. 255–288.

[19] M. KUCHARIK, M. SHASHKOV AND B. WENDROFF, *An efficient linearity-and-bound-preserving remapping method*, J. Comput. Phys., 188(2) (2003), pp. 462–471.

[20] M. SHASHKOV AND B. WENDROFF, *The repair paradigm and application to conservation laws*, J. Comput. Phys., 198(1) (2004), pp. 265–277.

[21] RL. LOUBERE, M. STALEY AND B. WENDROFF, *The repair paradigm: new algorithms and applications to compressible flow*, J. Comput. Phys., 211(2) (2006), pp. 385–404.